Secondary atomization of micrometric fuel droplets impinging onto heated targets

A. S. Moita[1,*], S. Sauer[1], A. L. N. Moreira[1]

1: IN+ - Department of Mechanical Engineering, Instituto Superior Técnico – TU Lisbon, Lisbon Portugal
* correspondent author: anamoita@dem.ist.utl.pt

Abstract The present work concerns the experimental description of the impact of micrometric droplet streams onto smooth and micro-structured surfaces, heated within a wide range of temperatures. The structural elements composing the surface micro-patterns are quadrangular pillars with side length *a* and height *h*. The distance between consecutive pillars is λ. Particular emphasis here is given in determining relations to predict the size of the secondary droplets generated under these conditions. Investigation of the impacts and the resulting secondary atomization was done combining phase-Doppler measurements and high-speed camera imaging and post-processing. The results show that within the nucleate boiling regime, the secondary atomization is mainly thermally induced, so the surface topography plays a secondary role. Within homogeneous wetting, the topographical micro-patterns leading to larger roughness ratio $r_f=(2a+\lambda)^2/[(2a+\lambda)^2+8ah]$ promote the generation of larger droplets. Hence the size of the secondary droplets is well related with $D_S/D_0=AWe^{-a}Re^{-b}Ja^{-c}.f(\delta_L)\ .f(r_f)$ where δ_L is the thickness of deposited film which could not be avoided in this boiling regime. Within the film boiling regime, the disintegration of the micrometric droplets over smooth surfaces is analogous to that of millimetric singe droplets. Hence the size of the secondary droplets can be estimated from the correlation proposed by Moita and Moreira (2009), $D_S/D_0=BWe^{-0.6}Re^{-0.23}$, which was derived for the impact of single millimetric droplets. Very good agreement was obtained between this correlation and data gathered from the present study and from the work reported by Müller *et al.* (2008a, b, 2009). However, in this regime the effect of the surface topography is more complex as it alters significantly the droplet dynamics. Hence, the correct scaling of surface topography is not solely a function of r_f. The exact relation was not found yet but the results suggest that optimized patterns (namely playing with the effect of λ) allow narrowing or widening the secondary droplet size distributions. This can be advantageous for the mixing and combustion processes in IC engines.

1. Introduction

Approaches to model the secondary atomization generated at the impact of a spray onto heated flat surfaces usually follow two paths; either they are based on an empirical approach based on integral or averaged parameters of a particular spray, thus completely lacking universality, or explore the thermal and hydrodynamic mechanisms observed at the impact of single millimetric droplets (Tropea and Roisman, 2005). Several studies, based on the latter approach have allowed developing several threshold criteria to predict the impact regimes in a quite suitable manner for many practical applications at ambient temperature, as extensively reviewed by Moreira *et al.* (2010). However, as also explained in Moreira *et al.* (2010) accurate relations to predict the secondary atomization (size and velocity of the droplets) are still a challenge, even for single droplet impacts. Then extrapolation to spray impact is in many cases very limited.

A mid-term between these approaches is recognized to be required, for instance considering the impact of sub-millimetric droplet streams, but very little work is still available in the literature and most of them are focused on the study of single droplet impacts above the Leidenfrost temperature (*e.g.* Rieber and Frohn. 1999, Karl *et al.* 1996), few exceptions made for instance to Naber and Farrel (1993) and to Richter *et al.* (2005). Additionally, the influence of surface properties (roughness, *wettability*) is far known to be important in both thermal and hydrodynamic behaviour of the impinging sprays, but just within the last decade the study of this effect was intensified for

single droplet impacts and only a few address micrometric droplet chains, exception made to Karl *et al.* (2000) and more recently to the work of Müller *et al.* (2008a, b, 2009). This is in fact a complex issue since the impact of sub-millimetric droplets cannot be simply extrapolated as a scaling exercise based on dimensionless numbers, since aerodynamic effects which are much less evident in milllimetric droplets strongly affect micrometric droplets (*e.g.* Moita *et al.*, 2001).

In this context, the present work concerns the experimental description of the impact of micrometric droplet streams on smooth and micro-structured surfaces, heated at different temperatures, to cover the various heat transfer regimes, from nucleate boiling to film boiling regimes. Particular emphasis is given in determining relations to predict the size of the secondary droplets generated under these conditions. This work is integrated in a wider project addressing the design of micro-structured surfaces to enhance heat transfer at liquid-solid interfaces. Popular application of micro-textured surfaces is in cooling applications. Some of them can be assessed based on single droplet impact, but in many others such as spray cooling, the liquid delivery is made using one or various droplet chains, which alters significantly the boundary conditions of the problem, so that a specific study of the hydrodynamic and thermal behaviour of the impact of sub-millimetric droplets must be addressed. In such applications secondary atomization is actually and unwanted phenomenon which must be controlled (*e.g.* Bertola and Sefiane, 2005), so it must be accurately described. Furthermore, the size distribution of the secondary atomization induced by thermal effects can provide important information on the heat transfer behaviour and therefore on the cooling performance (*e.g.* Moita and Moreira, 2012). Given the size of the droplets and the impact conditions studied here, the conclusions of the present work are expected to be useful in applications in IC engines, for which the accurate description of the secondary spray resulting from the impact of micrometric droplets is still a vital and unsolved issue.

2. Experimental method

2.1 Experimental arrangement

The experimental set-up mainly consists on a droplet generator (Model MDG100) producing single droplets and monodisperse streams, which were directed onto a heated surface placed at a distance of 100mm. The test surfaces are coupled on a copper block heated by 264W cartridge heaters. The basic set-up is schematically represented in Figure 1. To ensure stable impingement streams, while keeping the thickness of deposited liquid film under control, the droplet generator was used under very demanding working conditions, considering short duration impingement periods (ranging from a couple of milliseconds up to 1 second). Under these conditions it is difficult to keep the droplet stream always stable, so a reservoir was attached to a rotating disc, placed between the exit nozzle and the test surface, to displace the droplet stream when required (namely while it was unstable). Afterwards the disc is rotated and the stream can penetrate the orifice for a short time depending on the speed of the disc, thus impacting the target surfaces.

The millimetric droplets are generated at a tip of a tube with 0.9mm of internal diameter. The micrometric droplets are produced using orifices ranging between 50 and 100μm. A jet is created by forcing the liquid through the orifice. This jet would naturally break up into drops of different sizes. However, if a disturbance in form of a square wave at the appropriate frequency is applied to the reservoir, the jet breaks up into uniform drops at the rate of one drop per excitation cycle, leading to a stream of equally spaced monosized droplets. The excitation frequency was created using a Wavetek Model 191 frequency generator. Verification of the produced frequency was done with an oscilloscope to ensure that the settings corresponded to the correct frequencies.

Surface temperature of the targets is acquired using fast response thermocouples “Medtherm”. The thermocouples are 3mm apart, taking from the reference the thermocouple that is placed in the

center of the droplet impact region (r=0mm). They are aligned with the top of the surface where the impact occurs. Another embedded thermocouple is used to control the cartridge heaters, using a PMA KS20-I controller.

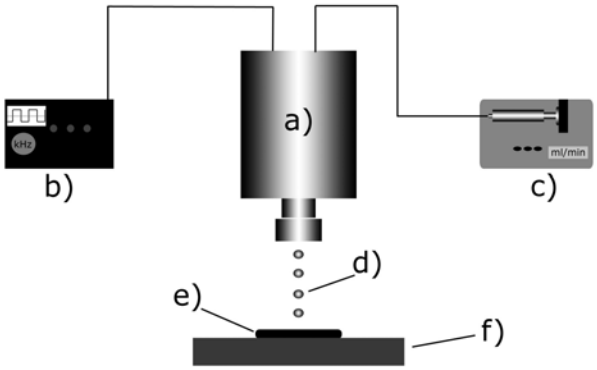

Fig. 1. Display of the schematic of the experimental set-up: a) droplet generator, b) frequency generator, c) syringe pump, d) droplet stream, e) test surface, f) heating block.

The signal of the thermocouples is sampled with a National Instruments DAQ board associated with a BNC2120 and amplified with a gain of 300 before processing. Different acquisition frequencies were used to characterize the temporal variation of the instantaneous temperature. Hence, to capture the entire variation along droplet deformation process, a relatively low frequency must be used (of the order of 2Hz). Then to refine the measures to particular instants a larger frequency was considered, of the order of 10kHz.

2.2 Measurement techniques and calibration procedures

Both an Image Acquisition System (IAS) and a Phase Doppler (PDA) System were used to characterize the impact dynamics and quantify the size and velocity of the droplets. The main element of the IAS is the high-speed camera (Phantom v4.2 from Vision Research Inc., with 512x512pixels@2100fps and a maximum frame rate of 90kfps). To record the impact history of the micrometric droplet streams the frame rate was varied between 2200 and 6300 fps (208 x 400 pixels). For the set-up used here, the resolution is 16μm/pixel. As in previous work with millimetric droplets, also here image post processing was used to characterize secondary droplet sizes between 40μm and nearly 1mm, while the Phase Doppler system allows to measure droplet sizes between 1μm and 250μm. The size distributions obtained by each technique are then combined to obtain an *extended-pdf* to evaluate secondary droplet sizes over the extended range comprised between 1μm and 1mm (*e.g.* as in Cossali *et al.*, 2005, Moreira *et al.*, 2007, Moita and Moreira, 2009).

The images were processed using home made routines and a macro designed within the software ImageProPlus. Several optimization processes were made to establish the correct intensity and threshold values to obtain reliable measurements. Several parameters such as maximum, minimum and average diameters as well as aspect ratios are evaluated in a post-processing routine. Detailed description of the post-processing basic procedures can be found in Cossali *et al.* (2005), Moreira *et al.* (2007) and Moita and Moreira (2009). The complete procedures and routines developed to treat images of the micrometric droplet arrays are presented in Sauer (2012).

To ensure that droplets are not counted two or three times, the time space between evaluated frames is enlarged. The effect of the time between frames was inferred for different combinations (*e.g.* every frame, every third or every fifth frame). For the distributions presented here, every third picture was evaluated, which was determined to be enough to avoid over counting. To calculate the intensity at a given time, all measurement files are evaluated for the same time step. The number of

counted droplets is then divided by the number of measurement files. The instant t=0 corresponds to the moment when the first primary droplet enters the measurement volume.
Slight variation of the total area of interest (AOI) occurred when evaluating droplet impacts over different surfaces due to variable set-up conditions. To quantify the inaccuracy associated to this variation of the AOI, secondary atomization is measured within two different areas: one is used to measure the primary droplets which do not influence secondary atomization measurement and the second represents the amount of measurement volume that is removed for the other condition. With an overall intensity of about 80 droplets in the later course of the impingement (t>20 ms), the inaccuracy related to the variation of the AOI is approximately 4 %, in the worse case scenario.

Significantly reliable frequency measurements (droplet counting) were obtained with the IAS. Although its spatial resolution allows the measurement of droplet sizes $D_s \geq 40\mu m$, large fluctuations for the measurements along time were observed for $D_s \leq 100\mu m$. Hence, most of the size distributions obtained with nucleate and transition boiling regimes are close to those obtained by the Phase Doppler system, while the influence of the large droplets detected by image analysis in the size distribution is only noticeable within the film boiling regime.

The Phase Doppler instrument is a two-component system from Dantec. This system is composed by a co-variance processor DANTEC 58N10 and a 300-400 mW air-cooled Argon Ion Laser from Spectra-Physics. The optical configuration is summarized in Table 1.

The scattering angle of 70° was chosen because it was observed to reduce the sensitivity of the measurements to the refractive index to a minimum (Pitcher and Wigley, 1991). Similar configurations were used by Cossali *et al.* (2005) and Moita and Moreira (2009, 2012) for the same reasons. The refractive indices are 1.334 for water and 1.359 for ethanol. The influence of the temperature on the refractive index was considered has in Moita and Moreira (2009).

To characterize the secondary droplets resulting from millimetric droplets, the control volume was positioned at r=0mm, z=2.5mm, and z=5mm. For the micrometric droplets, the control volume was located at 1.2 mm above the surface and at 1.2 mm lateral distance from the point of impingement. Keeping a lateral distance to the impingement area was necessary to avoid measuring primary droplets.

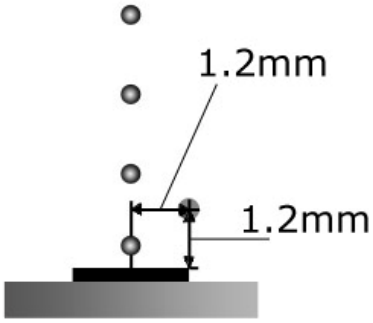

Fig. 2. Position of the measurement volume with respect to the point of impingement.

The size of the primary (and secondary) droplets larger than 200μm is mainly quantified based on high-speed visualization and image post-processing. For droplets smaller than 200μm both size and velocities were double checked by measurements with the Phase Doppler instrument.

To achieve a monodisperse droplet stream excitation frequency, flow rate and strobe light frequency were altered until a standing line of droplets appeared. Afterwards the uniformity of the generated droplet streams was verified with the PDA. If the majority of the droplets was found to be constantly with a diameter tolerance (±10μm) the measurement was considered valid. Figure 3 exemplifies a measurement of a constant diameter around 140 μm.

Table 1 Optical configuration of the phase Doppler instrument.

	Value
Transmitting optics	
Laser power [mW]	300
Wavelengths [nm]	514 and 488
Beam spacing [mm]	60
Transmitter focal length [mm]	310
Frequency shift [MHz]	40
Receiving optics	
Scattering angle [º]	70
Receiver focal length [mm]	310
Processor parameters	
U signal bandwidth [MHZ]	1.2
V signal bandwidth [MHZ]	0.4
S/N validation [dB]	0
Spherical validation [%]	10

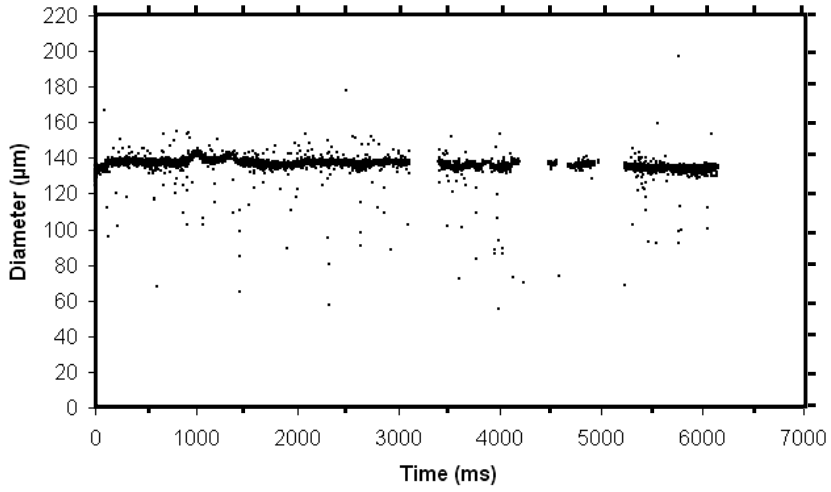

Fig. 3. Example of a primary droplet stream measurement which was considered valid (30000 valid samples within 6 seconds, Q=0.8 ml/min f_e=8000 Hz. PDA measurements were performed at r=0mm, z=50mm from the surface).

The measurements are further compared to those determined from the relation $D_0 = 6Q \cdot (\pi \cdot f_e)^{-1/3}$, with D_0 as droplet diameter, Q as flow rate and f_e as the applied excitation frequency. The agreement is fairly good in most of the cases. Larger disagreement is mainly attributed to instabilities of the stream. Only stable conditions were considered in the final measurements.

2.3 The target surfaces

The surfaces used here are made from a silicon wafer and are micro-patterned using square pillars as structural elements. The side length of the pillars is *a* and the height h. The distance between consecutive pillars is λ, as defined in Figure 4. All these distances are varied from 5µm up to 200µm. Such wide range of the size of the structural elements is required for the accurate scaling, which

depends on the size of the droplet and of the boundary conditions (*e.g.* dry *vs* wet surface).

The patterns are printed on the silicon wafer by lithography and processed by plasma etching. To reach higher pillars, the wafer surfaces were coated with aluminum, before the lithography. So, besides plasma etching, wet chemical etching is required for the aluminum coating. The micro-patterns are controlled to have known, precise values, using a profilemeter, with a measurement precision of 200Angstroms. Finally, the surfaces are checked by SEM/EDS analysis. Heterogeneity of the patterns was found to be lower than 3%. The wettability of the surfaces was also characterized, based on the static and dynamic contact angles, measured at room temperatures, inside a thermostatted ambient chamber (Ramé-Hart Inc., USA, model 100-07-00), using the Sessile Drop Method. An average value is considered for each pair liquid-surface which is determined from at least eight measurements taken at different regions of the surface. The time evolution of the average contact angles is obtained by curve fitting and the final values are determined by extrapolation. The detailed measurement procedure has been described in previous works (*e.g.* Moita and Moreira, 2012). The set of the surfaces used in this study is summarized in Table 2.

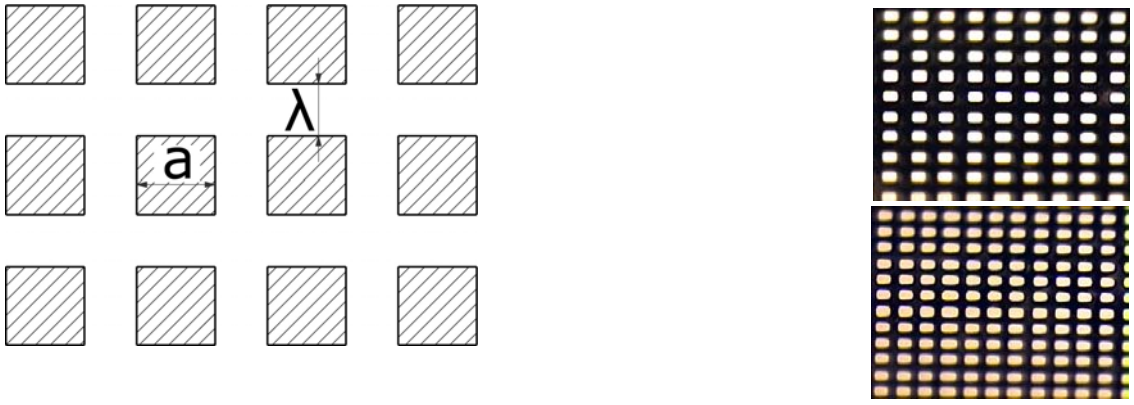

a) **b)**

Fig. 4. a) Definition of the dimensions *a*, *h*, and λ characterizing the topography of the micro-textured surfaces. b) Sample surfaces.

A homogeneous wetting regime is predicted for all pairs liquid-surface, according to the classical approach of Cassie and Baxter and of Wenzel theories. Additionally, during the measurement of the contact angles, a visual inspection of the droplets in contact with the surfaces was performed with an optical microscope, coupled with a CCD camera, also seems to confirm the occurrence of a homogeneous wetting regime for all the surfaces at room temperature, following the approach considered in Tata *et al.* (2011) and in Moita and Moreira (2012).

2.4 Working conditions

The working fluids are water and ethanol and were selected to allow exploring opposite wetting scenarios, which are known to strongly influence the thermal and hydrodynamic behaviour of the impacting droplets. Surface temperatures are varied within a wide range, between $T_{amb} \leq T_W \leq 310$ºC to cover all the heat transfer regimes, from natural convection to film boiling.

The boiling regimes are identified based on the visualization of the characteristic boiling morphologies and on the instantaneous temperature measurements obtained at the droplet-surface contact region, which are used to determine the overheating temperatures as defined in Richter *et al.* (2005) and later in Müller *et al.* (2008a). Table 3 summarizes the working conditions.

Table 2 Main topographical characteristics (defined in Figure 4) used in the customized micro-textured surfaces.

	a [µm]	h[µm]	λ[µm]	θ [º]
Smooth	≈ 0	≈ 0	≈ 0	86.0
S1	105	23.7	405	44.9
S2	190	23.3	311	60.7
S3	190	23.5	116	65.1
S4	307	23.7	334	61.5
S5	46	23.4	158	74.4
S6	162	23.1	397	50.6
S7	290	23.3	338	70.0
S8	211	23.5	201	65.6
S9	43	23.8	53	57.2
S10	146	23.4	50	92.7
S12	76	23.2	104	65.3
S12	225	23.9	80	70.7
S13	152	23.4	77	56

Table 3 Working conditions.

Millimetric droplets		
Liquid	**Water**	**Ethanol**
Primary droplet size - D_0 [mm]	3.1	2.6
Primary droplet velocity - U_0 [ms^{-1}]	1.4	1.4
Surface temperature – $T_{W,0}$ [ºC]	$T_{amb}< T_{W,0} <310$	$T_{amb}< T_{W,0} <260$
Micrometric droplets		
Liquid	**Water**	**Ethanol**
Primary droplet size - D_0 [µm]	$320<D_0<340$	$180<D_0<270$
Primary droplet velocity - U_0 [ms^{-1}]	$4.4<U_0<7.0$	$3.2<U_0<4.5$
Frequency - f_e[Hz]	$5000<f_e<9100$	$2100<f_e<5000$
Spacing - S [µm]	$180<S<580$	$940<S<1480$
Surface temperature – $T_{W,0}$ [ºC]	$T_{amb}< T_{W,0} <310$	$T_{amb}< T_{W,0} <260$

3. Results and discussion

Following the previous work of Moita and Moreira (2009, 2012) concerning the impact of single millimetric droplets onto hot, smooth and micro-textured surfaces, the results in this paper will focus on the characterization of the secondary atomization generated from the impact of micrometric droplet chains. The main objective is to scale down the observed mechanisms and particularly the relevant surface parameters to be considered in the design of smart interfaces to enhance hydrodynamic and thermal behaviour of droplets at the micro-scale. This is relevant given the numerous applications which actually deal with micrometric droplets, although most of the studies performed with enhanced micro-textured surfaces deal with millimetric droplets.

3.1 Nucleate boiling regime

As for single droplet impacts, the secondary atomization resulting from the impact of micrometric droplet chains is generated by diverse disintegration mechanisms, depending on the heat transfer

regime, so that the associated characteristics of size and velocity of the secondary droplets is significantly different within each regime (*e.g.* Richter *et al.*, 2005, Müller *et al.*, 2008a, b).

In the present paper, the impact of micrometric droplets on solid surfaces, within the nucleate boiling regime (overheating temperature $T_{\Delta}=T_{wall}-T_{saturation}=50°C$) was investigated for water and ethanol within a range of impact Weber numbers between $92<We<213$ for water and $73<We<216$ for ethanol. The frequency of the droplet generation required to assure a stable droplet stream was too high, so that liquid film deposition could not be avoided. Differences between water and ethanol are significant and are mainly due to the thermophysical properties of both liquids. Hence, the ethanol droplets completely wet the surface, given its low surface tension, leading to an enhanced liquid-solid contact, as illustrated in Figure 5a), for ethanol droplets impacting on a smooth surface at a low Weber number. Despite a few droplets can be generated by prompt splash, promoted by the wet surface boundary condition, most of the secondary droplets are clearly generated by thermal induced atomization, being mainly ejected in the axial direction. Similar behaviour is reported by Richter *et al.* (2005) and by Müller *et al.* (2008a, b). An influence of the impact Weber number has been found insofar as a higher impact Weber number leads to the formation of a wider and thinner deposited film, increasing the liquid-solid contact area (Figure 5b).

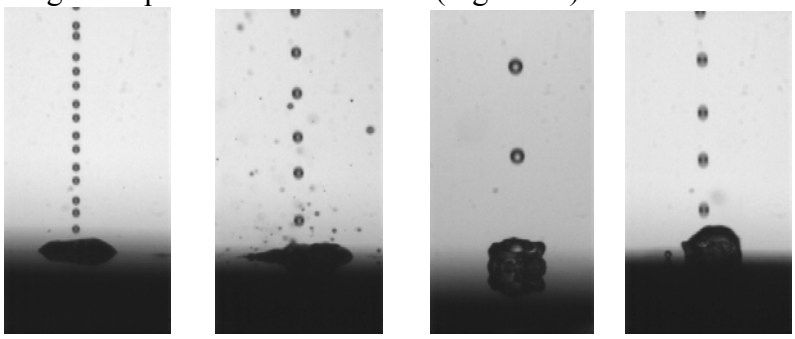

a) **b)** **c)** **d)**

Fig. 5 Comparison of the morphology of ethanol (a, b) and water (c, d) droplets impacting on a smooth surface at low and high Weber numbers, within the nucleate boiling regime. The surface is heated at $T_{\Delta}=50°C$ above boiling temperature. The images were taken at an instant After Impact, $t_{AI}=11ms$. Impact conditions: a) $D_0=180\mu m$, $u_0=3.2m/s$, $We=73$ b) $D_0=270\ \mu m$, $u_0=4.5m/s$, $We=216$ c) $D_0=340\ \mu m$, $u_0=4.4\ m/s$, $We=92$ d) $D_0=320\ \mu m$, $u_0=7\ m/s$, $We=213$.

Consequently, a more intense secondary atomization is observed at the early instants right after the impingement, as shown in Figure 6, for ethanol droplets.

Given the known limitations of accuracy of the number count measurements performed with the Phase Doppler instrument, as they are amplitude dependent, the number count N_S given in Figure 6 is mainly obtained from image post-processing.

On the other hand, the water droplets tend to keep a more oval shape, as the higher surface tension restricts the spreading of the lamella, even at higher Weber numbers (Figure 5c) and d)). This shape, which lessens the wetted area, associated to the much higher thermal properties of this liquid (namely the conductibility coefficient, the heat capacity and the latent heat of evaporation) enables the following droplets to cool the already deposited liquid successfully, thus preventing it from boiling, for the conditions studied here.

In summary, the thermal induced disintegration of micrometric droplets within the nucleate boiling regime is very similar to those described for millimetric droplets. In line with this, it is suggested that the thermal induced atomization to be well described with the correlation proposed in Moita and Moreira (2009), although in this case, the effect of the film thickness of deposited liquid δ_L must be taken into account. So, the relation:

$$SMD/D_0=AWe^{-a}Re^{-b}Ja^{-c}.f(\delta_L) \qquad (1)$$

is suggested here. A is a fitting constant, SMD is the Sauter Mean Diameter of the secondary droplets and $Ja=C_p\ (T_w-T_{boiling})/h_{fg}$ is the Jacob number, being C_p the specific heat, and h_{fg} the latent heat of evaporation. Actual fitting to the experimental data is not considered yet, as the liquid film thickness was not evaluated either here or in similar studies. This is work in progress.

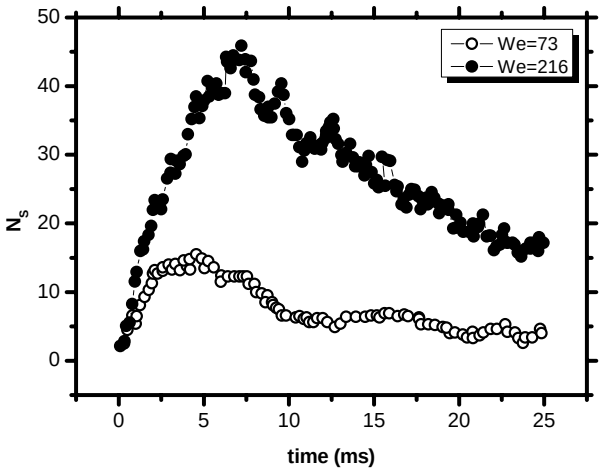

Fig 6. Number of secondary droplets, N_S, resulting from the impact of ethanol droplets impacting on a smooth surface at different Weber numbers, within the nucleate boiling regime. The surface is heated at T_Δ=50°C above boiling temperature.

Effect of surface topography

Given that the secondary atomization is mainly thermally induced in the deposited droplets and film, the effect of the surface topography is minor, even considering rough scales which are relevant when compared to the thickness of the film, as suggested by Vander Wall *et al.* (2006). Thus the mild effect of the surface topography is mainly to allow an earlier triggering of the thermal induced atomization, as a result of the increase of the contact area. This earlier triggering results in the deviation of the secondary droplets size distribution obtained from PDA measurements, to smaller diameters, as shown in Figure 7, for ethanol droplets.

Similar behaviour is observed for water droplets, being particularly evident the effect of the surface topography particularly between the smooth surface and surface S13, which has larger liquid-solid contact area. The results depicted here focus on the surfaces in which a, h and λ are smaller/or of the order of magnitude of the primary droplets. However, a finer scaling is still required, particularly for impacts onto dry surfaces.

From the discussion presented so far, it is fare to establish a qualitative comparison with single droplet impacts, to identify the relevant parameters to proceed with the optimization of the surface patterns. So, as for millimetric droplets, the secondary atomization within the nucleate boiling regime, for the impact conditions studied here is mainly thermally induced. In a recent study, Moita and Moreira (2012a,b) refer that the homogeneous wetting regime, the patterns promoting heat transfer will trigger the thermal induced atomization to occur earlier and give rise to droplets with larger sizes and higher ejecting momentum, as a result of the more intense boiling. Such patterns will have larger roughness ratio $r_f=(2a+\lambda)^2/[(2a+\lambda)^2+8ah]$. Hence, for homogeneous wetting regimes, rf should be well related with the secondary droplet sizes, both for millimetric and micrometric droplets. This trend is suggested by the results depicted in Figure 8.

In line with this, the final relation describing the size of the secondary atomization in these conditions should be in the form:

$$D_S/D_0=AWe^{-a}Re^{-b}Ja^{-c}.f(\delta_L)\ .f(r_f) \qquad (2)$$

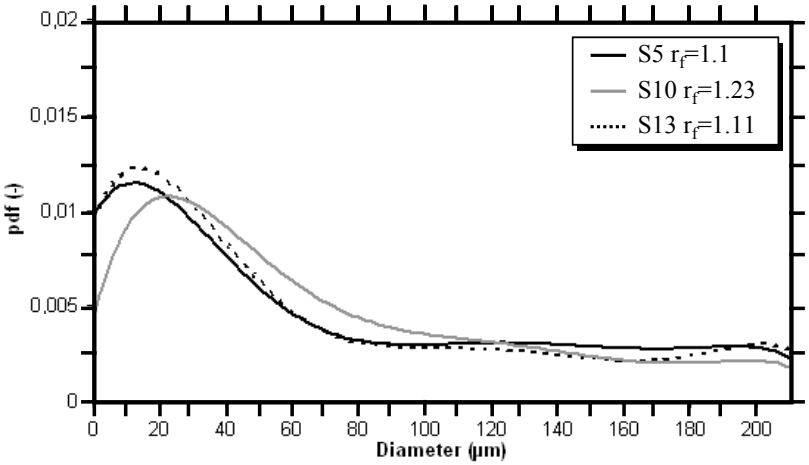

Fig. 7. PDF of the secondary droplet size distribution resulting for impact of micrometric ethanol droplets (D_0=180µm, u_0=3.2 m/s) over the micro-textured surfaces, within the nucleate boiling regime (T_Δ=50°C)**.** PDA measurements were performed at r=1.2mm, z=1.2mm.

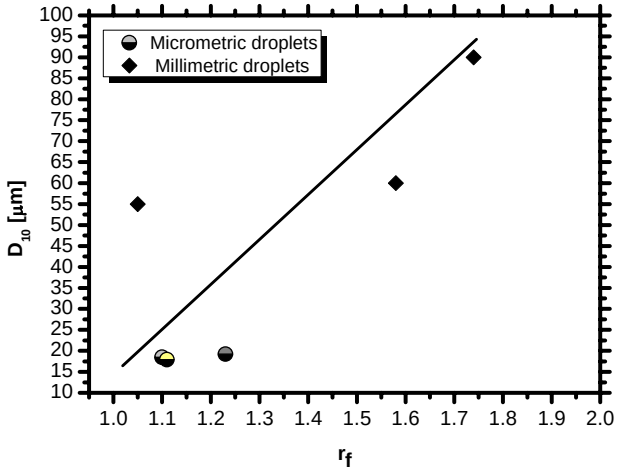

Fig. 8. Relation between r_f on the size of the secondary droplets (obtained from the PDA measurements) resulting from thermal induced atomization of micrometric and millimetric ethanol droplets impacting onto the silicon surfaces, within the nucleate boiling regime.

3.2 Film boiling regime

T_Δ=80°C is already clearly within the transition regime for ethanol droplets, while water requires a slightly higher overheating. However, transition boiling turned out to be very difficult to analyse for both liquids, given the non-reproducible effects observed at droplet impact morphology, which are attributed to the unstable wetting conditions, characteristic of this regime.

Much more reproducible behaviour is observed within the film boiling regime, which was observed for both water and ethanol at T_Δ=120°C. Aerodynamic effects associated to strong vapour pressure forces promote the fast levitation of the droplets from the surface. Now, the droplets impact on the surface already dry and prompt disintegration is the dominant mechanism. The impact outcomes are clearly dependent on the Weber number: complete levitation without break-up occurs at lower We, while an increasing number of secondary droplets is observed at successive higher We.

This behaviour is similar for both water and ethanol droplets, although break-up is more difficult for water droplets, as expected. Nevertheless the break-up of the droplets is clearly induced by inertial effects, so that besides the Weber number also the Reynolds number is expected to play an important role. This is due to the fact the size of the droplets is strongly related with the thickness of the lamellas, which can be scaled as $h_L \sim (\nu D_0/u_0) = D_0 Re^{-1/2}$. Hence, the mechanism here

is clearly equivalent to that observed at millimetric droplet impacts, so the size of the secondary droplets should be well described with the relation proposed by Moita and Moreira (2009):

$$D_S/D_0=BWe^aRe^b \quad (3)$$

where a=-0.6 and b=-0.23 are negative exponents, indicating that viscosity and or surface tension contribute to the generation of larger secondary droplets. Fitting of this relation with the present results is depicted in Figure 9, together with an alternative correlation proposed by Müller *et al.* (2008a), solely based on the Reynolds number.

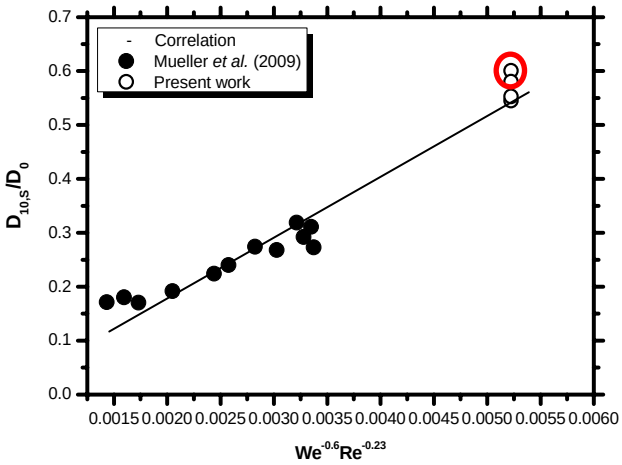

a)

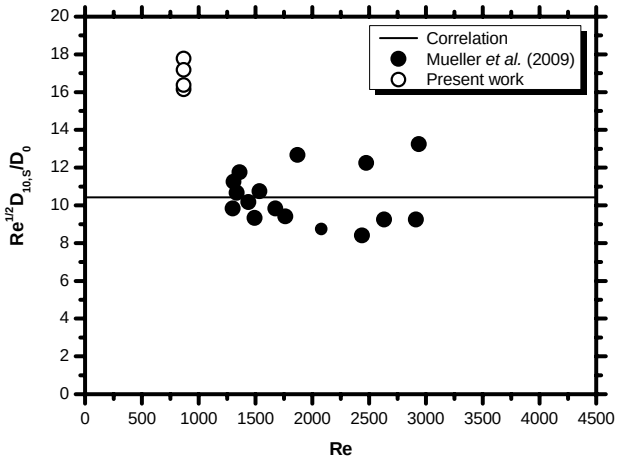

b)

Fig. 9. Average diameter of the secondary droplets generated at the impact of a monosize stream within the film boiling regime, scaled as **a)** a function of both We and Re numbers, **b)** solely function of the Reynolds number. The figure gathers data reported by Müller *et al.* (2008a, b, 2009) with those of the present work. The liquid used by Müller *et al.* (2008a, b, 2009) is iso-octane (D_0=81 μm, 4.5<u_0<21.7 m/s). The liquid used in the present work, for this set of results is ethanol (D_0=270 μm, u_0=4.5 m/s).

The Figure evidences the important role of the Weber number in the disintegration process, providing good fitting between equation (3) and the experimental data. The Reynolds number alone is not enough to describe the process. The discrepancy highlighted with the circle is due to the

effect of surface topography which is not taken into account.

Effect of surface topography

Now, the chosen roughness pattern has an evident influence on the secondary atomization. This is clear looking at the droplet morphology, depicted in Figure 10. It can be observed that on the smooth surface the liquid spreads after the impingement and a wide lamella is created which is levitated at the rims. In the impingement zone however the liquid is not levitated and the following droplet impinges on the existing film. Secondary droplets are created as a consequence of the impingement on the liquid film and the chaotic disintegration of the boiling lamella in the impingement zone. This naturally leads to a wider spectrum of secondary droplet sizes. On the structured surfaces the impinging liquid performs a prompt splash. There is no wide-spreading lamella but a complete disintegration of the impinging droplet. Due to the surface roughnes,s no stable lamella is formed in the impingement area and the small droplets that were created in the course of the splashing are levitated completely and leave the impingement area. Consequently the subsequent droplets also encounter a rough surface and perform a prompt splash.

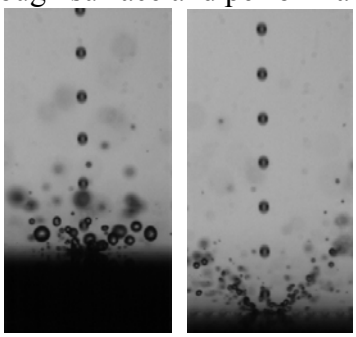

a) **b)**

Fig. 10. Effect of surface topography in the disintegration process within the film boiling regime. Ethanol droplet stream (D_0=270 μm, u_0=4,5 m/s) impacting onto **a)** a smooth silicon wafer surface, **b)** a micro-textured silicon wafer surface (S17: λ=77μm, h=23.4 μm, a=152 μm) within the film boiling regime (T_Δ=120°C/T_w =200°C).

The smooth surface clearly gives rise to larger droplets while the rough surfaces promote the secondary atomization to occur earlier and with significantly smaller droplets. This is due to the fact that the structural elements act to promote hydrodynamic disintegration which overcomes the thermal induced one, so that the rougher surface leads in fact to smaller secondary droplets. The resulting distributions are shown in Figure 11.

To introduce the correct scaling of surface topography in equation (3), one must be able to include both thermal and hydrodynamic effects so, that the effect of surface topography is not solely a function of r_f. In fact the amplitude of the structural elements is already weighted in r_f, but the effect of the distance between peaks may now act as a destabilizing or smoothing effect which is not accounted by the roughness factor. Hence, for the patterns where the distance between the structural elements is sufficiently smal, a “smoothing” effect is observed and the disintegration is governed by thermal effects, giving rise to larger secondary droplets. On the other hand, as the structural elements are more apart they will naturally promote the disintegration of the lamella giving rise to a higher number of small secondary droplets, in a disintegration process which is dominated by hydrodynamic effects. This results in the narrowing of the size distribution (Figure 11).

Further research is now required to tune the adequate distances between peaks which endorse dominance of the thermal or of the hydrodynamic effects in the disintegration mechanisms, which will allow to control the size distribution of the secondary droplets, widening or narrowing them, respectively. However, this possibility of changing the secondary droplet size distributions brings

the opportunity to control the mass that is removed from the surface by secondary atomization in cooling applications. Another obvious application is in fuel injection systems, since the possibility to narrow or widen the size distribution of the secondary sprays is advantageous for the mixing and for the combustion processes in IC engines.

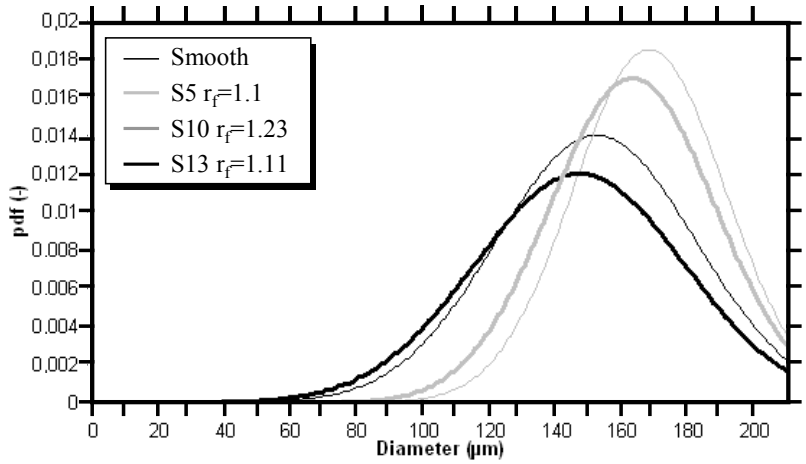

Fig. 11. Secondary droplet size distribution generated at the impact of a monodisperse stream of ethanol droplets (D_0=270 µm, u_0=4,5 m/s) onto various surfaces at T_Δ=120°C/T_w =200°C. (Phase Doppler measurements performed at r=1.2mm, z=1.2mm).

4. Final remarks

The present paper addresses the study of the dynamic and thermal behaviour of micrometric droplets impacting onto smooth and micro-textured surface, heated within a wide range of temperatures. Main focus is put on determining relations to predict the size of the secondary droplets generated under these conditions. Investigation of the impacts and the resulting secondary atomization was done combining phase-Doppler measurements and high-speed camera imaging and post-processing.

The results show that within the nucleate boiling regime, the secondary atomization is mainly thermally induced, so the surface topography plays a secondary role. Within homogeneous wetting, the topographical micro-patterns leading to larger roughness ratio $r_f=(2a+\lambda)^2/[(2a+\lambda)^2+8ah]$ promote the generation of larger secondary droplets (Fig.1), whose size is well related with $D_S/D_0=AWe^{-a}Re^{-b}Ja^{-c}.f(\delta_L)\ .f(r_f)$, where δ_L is the thickness of deposited film which could not be avoided in this boiling regime.

Within the film boiling regime, the disintegration of the micrometric droplets over smooth surfaces is analogous to that of millimetric singe droplets. Hence, the size of the secondary droplets can be estimated from the correlation proposed by Moita and Moreira (2009), $D_S/D_0=BWe^{-0.6}Re^{-0.23}$, which was derived for single droplet impacts. Very good agreements was obtained with data gathered from the present study and from the work reported by Müller *et al.* (2009), as depicted in Fig. 2. However, in this regime the effect of the surface topography is more complex as it alters significantly the droplet dynamics. Hence, the correct scaling of surface topography is not solely a function of r_f. The exact relation was not found yet but the results suggest that optimized patterns (namely playing with the effect of λ) allow narrowing or widening the secondary droplet size distributions.

5. Acknowledgements

A. S. Moita is grateful to Fundação para a Ciência e a Tecnologia (FCT) for supporting her through the Post-Doc Fellowship (REF:SFRH/BPD/63788/2009).

References

Bernardin, J. D., Mudawar, I. (1999) The Leidenfrost point: experimental study and assessment of existing models. Trans. ASME, 121:894-903.

Bertola, V., Sefiane, K. (2005) Controlling secondary atomization during drop impact on hot surfaces by polymer additives. Phys. Fluids, 17, 108104.

Cossali, G. E., Marengo, M., Santini, M. (2005) Secondary atomization produced by single drop vertical impacts onto heated surfaces Exp. Thermal Fluid Sci., 29: 937-946.

Kannan, R., Sivakumar, D. (2007) Impact of liquid drops on a rough surface comprising microgrooves. Exp. Fluids., 44(6):927-938.

Karl, A., Anders, K., Rieber, M, Frohn, A., (1996) Deformation of liquid droplets during collisions with hot walls: experimental and numerical results. Part. Syst. Charact. 13, 186-191.

Karl, A., Frohn, A. (2000) Experimental investigation of interaction processes between droplets and hot walls. Phys. of Fluids, 12:785-796. Moreira, A. L. N., Moita, A. S., Panão, M. R. (2010) Advances and challenges in explaining fuel spray impingement: how much of single droplet impact research is useful? Progress in Energy and Combustion Science, 36:554-580.

Moita, A. S., Moreira, A. L. N. (2009) Development of empirical correlations to predict the secondary droplet size of impacting boiling droplets. Experiments in Fluids, 47:755-768.

Moita, A. S., Moreira, A. L. N. (2012) Scaling the effects of surface topography in the secondary atomization resulting from droplet/wall interactions. Experiments in Fluids, 52(3):679-695

Moita, A.S., Roth, N., Gomaa, H., Weigand, B., Moreira, A.L.N. (2011) "Effect of the properties of the surrounding gas on the dynamic behaviour of bouncing droplets on a solid surface", 24th Annual Conference on Liquid Atomization and Spray Systems ILASS-2011, Estoril, Portugal.

Moreira, A. L. N., Moita, A. S., Cossali, G. E., Marengo, M., Santini, M. (2007) Secondary atomization of water and isooctane drops impinging onto tilted heated surfaces. Experiments in Fluids, 43:297-313.

Müller, A. Dullenkopf, K., Bauer, H.-J. (2008a) Application of an extended particle tracking method to analyze droplet wall interactions. Proc. 14th Int. Sym. Appl. Laser Tech. Fluid Mechanics, Lisbon Portugal.

Müller, A. Dullenkopf, K., Bauer, H.-J. (2008b) Analysis of droplet wall interactions with graded surface roughness. Proc. 22nd Int. Conf. Liquid Atomization and Spray Systems, ILASS-2008, Como Lake, Italy, 2008.

Müller, A. Velios, E., Dullenkopf, K., Bauer, H.-J. (2009) From single droplet to spray wall interaction – multiple droplet chains. Proc. 11th Triennial Int. Conf. Liquid Atomization and Spray Systems, ICLASS2009, Vail, Colorado, U.S.A.

Naber, J. D., Farrel, P. (1993) Hydrodynamics of droplet impingement on a heated surface. SAE Paper 930919.

Pitcher, G., Wigley, G. (1991) Sensitivity of drop size measurements by Phase Doppler anemometry to refractive index changes in combusting fuel sprays, in the Proc. 5th Int. Symp. Appl. Laser Tech. Fluid Mechanics, Lisbon, Portugal, 1990, Edited by Adrian, R. J., Durão, D. F. G., Durst, F., Maeda, M., Whitelaw, J. H., Springer-Verlag Berlin, Heidelberg, Germany, 1991

Randy L. Vander Wall, G., Berger, G. M., Mozes, S. D. (2006c) The combined influence of a rough surface and thin fluid film upon the splashing threshold and splash dynamics of a droplet impacting onto them. Exp. Fluids, 40:23-32.

Richter, B., Dullenkopf, K., Bauer, H.-J. (2005) Investigation of secondary droplet characteristics produced by an isooctane drop chain impact onto a heated piston surface. Exp. Fluids, 39:351-363.

Rieber, M., Frohn, A. (1999) A numerical study on the mechanism of splashing. Int. J. Heat Fluid Flow, 20:455-461.

Sauer, S. (2012) Characterization of the secondary atomization and thermal behaviour of a micro-droplet stream onto heated and enhanced surfaces. Thesis for the conclusion of the Bachelor in Aerospace Engineering, Universitaet Stuttgart.

Tata, M., Moita, A.S., Moreira, A.L.N. (2011) "Study of the effect of the topographical length scales on the wettability as strategy to control the interfacial phenomena at droplet-wall interactions", 24th Annual Conference on Liquid Atomization and Spray Systems, Estoril, Portugal.

Tropea, C., Roisman, I. (2006) Spray/wall interaction: how much physics do we need in our models? Proc. 6th World Conf. Exp. Heat Transf., Fluid Mech. and Thermodynamics, Matsushima, Miyagi, Japan.